

# Study on Startup Characteristics of Heat Pipe Cooled Space Reactor

**Yuan Yuan, Jianqiang Shan, Bin Zhang\*, Junli Gou, Bo Zhang**  
School of Nuclear Science and Technology, Xian Jiaotong University  
No.28, Xianning West Road, Xi'an, Shaanxi, 710049, P.R. China

## ABSTRACT

Future exploration of deep space requires space power with high power density, light weight, low cost and high reliability. Space reactor is an excellent candidate with its unique characteristics of high specific power, low cost, strong environment adaptability and so on. Among all types of space reactors, heat pipe cooled space reactor, which adopts the passive heat pipe as core cooling component, is considered as one of the most promising choice and is widely studied all over the world. Startup characteristics of this type space reactor are an active topic.

Previous studies mainly focused on the startup from high temperature rather than environmental temperature. In order to simulate the transient startup process from frozen state, a transient analysis code (TAPIRS) for heat pipe cooled space reactor power system (HPS) has been developed and applied to investigate the system transient performance during a startup from zero cold power to full power. The code integrates separately validated point reactor kinetics model, lumped parameter core heat transfer model, combined heat pipe (HP) model (self-diffusion model, flat-front startup model and network model), energy conversion model of alkali metal thermal-to-electric conversion units (AMTEC), and HP radiator model. By adjusting the control drum's rotational speed, the reactor can start up from subcritical state to full power state while the heat pipe, AMTEC from solid state to normal operational state.

*Key Words:* Space reactor; Heat pipe; AMTEC; Startup

## 1 INTRODUCTION

Over the past 60 years, extensive studies have been conducted on space reactors. The space reactor can be a thermal, an epithermal or a fast neutron spectrum reactor, while large power reactor often adopts a fast neutron spectrum design. A fast neutron spectrum nuclear reactor can be applied with different cooling systems, such as liquid metal HPs, circulating liquid metal or noble gas binary mixture of He-Xe [1]. The energy conversion technologies include dynamic and static energy conversion, namely: TE, AMTEC, free-piston stirling engines (FPSEs), thermionic (TI) energy conversion, or single-shaft, centrifugal flow turbo-machines.

Compared with other types of space reactor system, HPS is more promising and widely studied all over the world, which adopts the passive HP as core cooling component. The HP is essentially constant temperature device, which reduces differential expansion stresses within the fuel pins and supports structure. Other potential positive attributes of HPS include modularity, testability, simplified system integration, passive, and the elimination of single-point failures.

Reactor concept being developed for demonstration SAIRS [2] is coming from the NASA's Nuclear Systems Initiative (NSI) program. The concept applies Na-HPs that are integral with the reactor fuel pins and coupled to an AMTEC units. The HPs are used as the heat sink of the reactor. The HPs are also applied as integral parts of the HPS in other designs, such as SAFE-400 [3] and HP-STMCs [4]. The SAFE-400 is a 400-kWt reactor that has been designed to couple with a 100-kWe Brayton power, and use the HPs to carry the heat to an ex-core HP-to-gas heat exchanger system. HP-STMC is a HP cooled

---

\* Corresponding author. Tel.: +86 029 82663769; fax: +86 029 82663769

E-mail address: E-mail:binzhang@xjtu.edu.cn

nuclear reactor, similar to that of SAIRS. It has been developed and integrated to STE energy conversion modules and a HPs radiator in the HP-STMCs space reactor power system. The primary difference among these three concepts is the thermo-electric converters.

Most of previously published studies carried out only steady-state analysis, which is fundamental for reactor design. Wu et al. [5] proposed a new AMTEC analytical model, however did not couple with the power, flow rate and temperature of the working fluid. El-Genk and Tournier [2] presented his design of SAIRS and gave several key parameters, including the temperature changes and the operation range of the HP. Furthermore, Tournier and El-Genk presented a UNM HP model for steady-state performance prediction of the operation design limits of the HP. For transient analysis, El-Genk [6] presented the transient simulations results of the SCoRe-TE space power system during a reactor startup and transients following the electrical load demand. King and El-Genk [7] analyzed the thermal hydraulic characteristics of the submersion-subcritical, safe space (S4) reactor. Wright and Houts [8] described the results of a system code (PKHPID) capable of modeling the coupling between the reactor kinetics and heat pipe controlled heat transport. Ran et al. [9] performed a transient analysis for a 200 kW advanced space fast reactor RAPID-L. Most of the space reactor studies focused on alkali metal cooling space reactor which starts from the high temperature (alkali metal working in a liquid state), while the HPS startup needs more attention.

More attention is needed for the transient analysis of the frozen startup process of HPS. In order to simulate this transient process, a transient analysis code TAPIRS including the point reactor kinetics model, the lumped parameter core heat transfer model, three models for the HP system for different HP startup stages, energy conversion model of AMTEC, HP radiator model, and other basic components of a space reactor was established, which could analyze different stages in the startup process. The startup process starts from room temperature. As reactor power increases, HP and AMTEC will go through solid, melting, gas-liquid two-phase, eventually steady state operation. The whole process is complicated in thermal-hydraulic dynamics. The purpose of this paper is to present the results of a systems code capable of modeling the heat transport process in HPS based on SAIRS, which is complex and highly system dependent.

## 2 SYSTEM DESCRIPTION

El-Genk and Tournier [2] presented their design for the SAIRS power system. In this system a fast neutron spectrum nuclear reactor is cooled with a Na-HPs, and 18×5.6kWe Na-AMTEC units. The AMTEC units are divided into six blocks of 3 units and each block is cooled by K-HPs in a separate radiator panel. The AMTEC units, placed behind the radiation shadow shield, are heated by sodium HPs. The six AMTEC blocks in the power system are connected electrically in parallel. SAIRS has a nominal electrical power of 110kWe that is delivered at a terminal voltage of 400 V DC. The SAIRS HP-cooled nuclear reactor is comprised of 60 fuel modules. Each fuel module consists of three uranium nitride (UN), rhenium (Re) clad fuel pins arranged in a triangular lattice.

## 3 DESCRIPTION OF SYSTEM MODELS FOR HPS (TAPIRS)

Figure 1 shows the schematic diagram of this space reactor. A system code named TAPIRS was developed to study the transient characteristic of the HPS, which was written in Fortran 90 and consisted of a number of separate subroutine modules for:

- the point reactor kinetics model
- the lumped parameter core heat transfer model;
- the combined HP model (the self-diffusion model, the flat-front startup model and the network model);
- the energy conversion model for AMTEC;

- the HP radiator model.

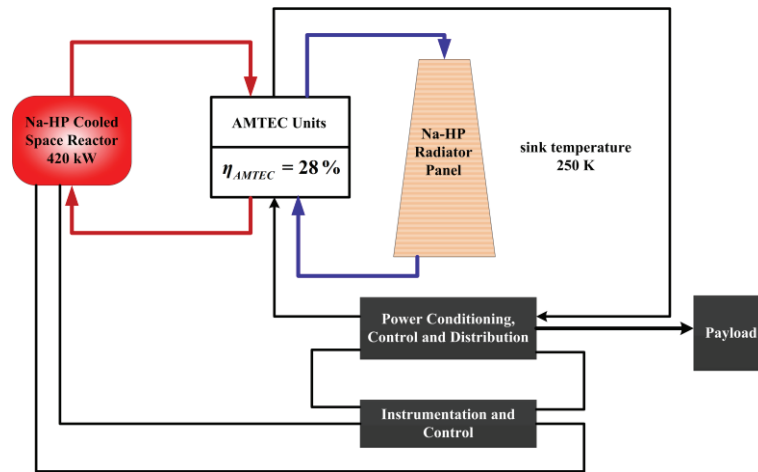


Figure 1 Schematic figure of primary and secondary HP loops of HPS

**Point reactor kinetics model:** The standard point reactor kinetics equations with six delayed neutron groups are solved to determine the reactor power given a specified input reactivity. The total reactivity is determined by including the core average temperature feedback effect [10]. The end floating method with high-order polynomial approximation [11] for solving the point reactor neutron kinetics equations.

**Core heat transfer model:** The cladding along the active length of the fuel pins in SAIRS is brazed to a central Mo-14%Re/Na-HP, as shown in Figure 2. For the convenience of calculating heat transfer between HP and the fuel pins, the triangle region is simplified as an annular layer surrounding the clad, and its thickness is calculated based on the triangle area. Therefore, the fuel rod is composed of four layers: fuel pellets, gap, clad and imagined outer wall respectively. Lumped-parameter models [12] can be used for the prediction of transient conduction in nuclear reactor components because of UN fuel's good heat transfer characteristics. Different from Wulff's model, the governing equation of imagined outer layer should be added. The process of transient, axisymmetric radial conduction through the fuel pellet, gap, concentric clad and imagined outer layer is shown in Figure 2. Fourth-Order Runge-Kutta scheme is used to solve the fuel temperature differential equations.

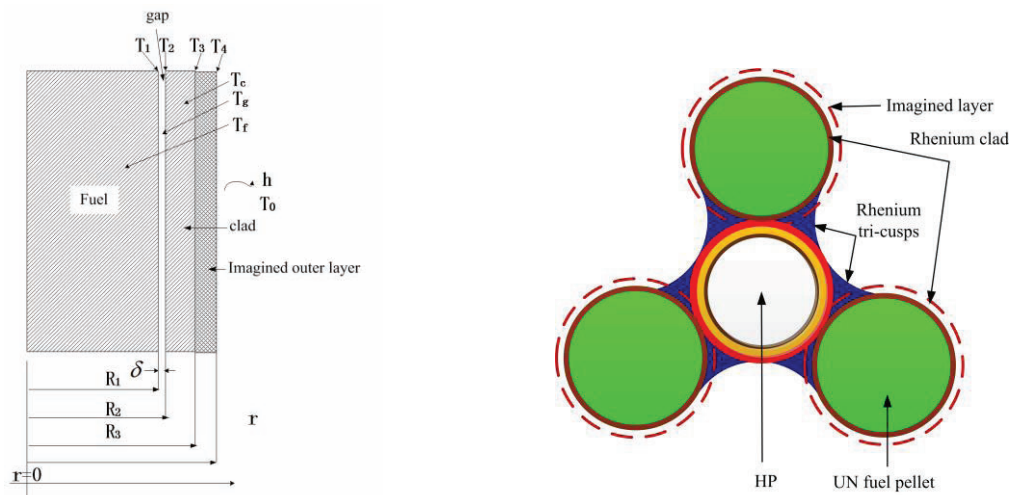


Figure 2 Geometry for fuel element

**Combined HP model:** HP usually consists of wall, porous wick, and vapor core. In order to reduce the circulation pressure drop, the space reactor adds a liquid annulus, as shown in Figure 3. Therefore, the wick is separated from the wall by an annulus filled with working liquid. The startup process of a liquid metal HP from the frozen state may be divided into several phases for the convenience of analysis. Enormous work has been devoted on the mathematical formulation of every HP Phase. This paper incorporates them into one model based on these mature models, as shown in Table 1.

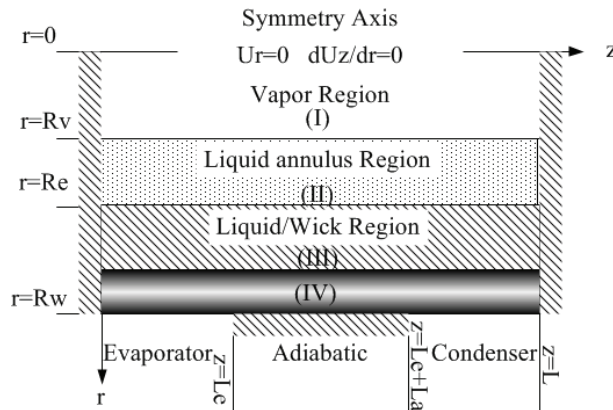
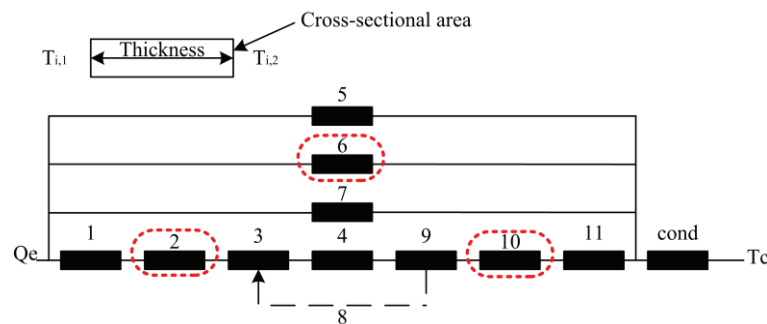


Figure 3 HP physical model and boundary conditions

Table 1 The HP models

Model	Startup Phases	References
The self-diffusion model	1-3	Ochterbeck J(1997)[13]
The flat-front startup model	4	Y.Cao(1993)[14]
The “network” model	5	ZUO(1998)[15]

Figure 4 illustrates the network of the heat transfer between the evaporator and the condenser. The existence liquid annulus makes the modeling of the HP adopted here unique. Because of adding a liquid annulus, the network model adds three thermal resistances which are evaporator liquid annulus radial direction thermal-conduction resistance (2 in Figure 4), adiabatic liquid annulus radial direction thermal-conduction resistance (6 in Figure 4) and condenser liquid annulus radial direction thermal-conduction resistance (10 in Figure 4). The mathematical formulation of the HP modeling should make the change correspondingly.



$Q_e$ -Evaporator heat input; 1-Evaporator wall (radial direction); 2-Evaporator liquid annulus (radial direction); 3-Evaporator wick (radial direction); 4-Vapor flow (heat convection); 5-Adiabatic wick (axial direction); 6-Adiabatic liquid annulus (radial direction); 7-Adiabatic wall (axial direction); 9-Condenser wick (radial direction); 10-Condenser liquid annulus (radial direction); 11-Condenser wall (radial direction); Cond-Convective cooling condition (condenser outer surface).

Figure 4 A one-dimensional heat conductor

For the alkali metal high temperature HP, seven heat transfer limitations should be considered. Five of them are physical factors limiting the heat flux in HP: the viscous limit, the sonic velocity limit, the entrainment limit, the boiling limit and the capillary limit. There are four limits include frozen startup limit, viscous limit, continuous flow limit and sonic limit must considered in the startup condition [16].

**AMTEC model:** Tournier [17] conducted a number of AMTEC design studies and steady-state analysis. The high performance AMTEC Model consists of four, interactively coupled sub-models: (a) Pressure loss model; (b) Electrochemical model; (c) Electrical model; (d) Thermal model. For the transient analysis of the AMTEC, the components temperature, working fluid flow rate, and heat transfer should be coupled. In this paper we add the transient temperature equation to calculate the evaporator and condenser temperature in AMTEC.

**Radiator model:** Each radiator panel has two sections that are thermally coupled using six, double vapor cavity K-HP. Lumped-parameter models can be used for the prediction of transient conduction in radiator panel.

#### 4 TAPIRS CODE DESCRIPTION

The TAPIRS code is divided into three modules: input module, calculation module, and output module. The flow chart is shown in Figure 5.

Before calculation, the code will initialize the input card and the transient initialization conditions including the reactor startup, AMTEC failure, the Na-HP failure, the control drum failure or partial loss of radiator heat transfer. When the transient condition is triggered, the code starts to initialize the system parameters, including the temperature, voltage and current of AMTEC, and the system power distribution. Then the code starts the transient calculation. According to the reactor insertion reactivity curve defined by the input card, the reactivity feedback module calculates the total reactivity. Then the point reactor neutron kinetics module can get the fast reactor fission power. The core thermal module calculates the temperature of fuel, gas gap and cladding, and determines safety limit on maximum fuel axial temperature under accident conditions. After the heat transferred from core to Na-HP under specific temperature difference is calculated, the Na-HP module can be called to calculate the HP startup or transient process.

The AMTEC module calculates a variety of cell parameters, the parameter value at the end of this time step will be used as the initial value for the next step.

The output of TAPIRS includes all system operation parameters, namely:

- 1 The reactor thermal power and temperatures;
- 2 The AMTEC electric power, current and temperatures;
- 3 The system efficiency;
- 4 The Na-HP temperatures and limits;
- 5 The emitted thermal power and temperatures of the radiator;
- 6 The total and feedback reactivities in the reactor core.

The rate and magnitude of the external insertion reactivity in the reactor, which are functions of the angular speed and rotation angle of the B<sub>4</sub>C/BeO control drums in the radial reflector, are necessary for the dynamic simulation. With these, the dynamic simulation can accurately mimic the transient operational process of the actual system. The results of such simulation are invaluable to the system designers, because they provide important information on the coupling effect from various components to

the overall system performance.

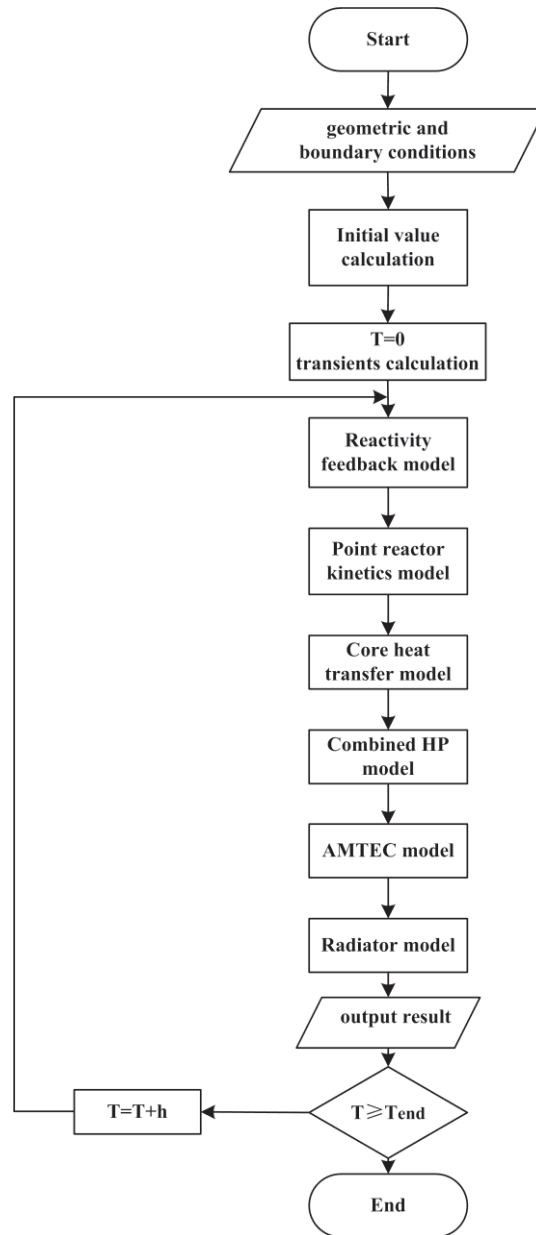


Figure 5 Flow chart of TAPIRS

## 5 STARTUP PROCEDURE

The USA SNAP-10A in 1965 [18] and the Russian TOPAZ-I systems in 1989 [19] both presumed that the power system will be heated electrically on the launch pad to a high enough temperature (i.e. 800 K), such that when the system is deployed in orbit its temperature will be above the freezing temperature of the liquid metal coolant (Na-K). Such an approach eliminates the need for a thaw system, and there is also no prior experience on thawing a liquid metal nuclear power system.

Because of the lack of paper which is analyze HPS startup procedure, the whole system startup

procedure has not been validated, but the component models has been validated with the references. The point reactor kinetics model was compared with Yuan and Hu[11], the lumped parameter core heat transfer model was compared with Wuff[12], the combined HP model was compared with El-Genk etc.[13-15] and the energy conversion model for AMTEC was compared with El-Genk etc.[2]. The specific validation work can be seen in the report[20].

This section of the paper describes a startup scenario for SAIRS. The input and results of the startup sequence are illustrated in Figure 7-15. Particular attention has been given to studying the startup characteristics of SAIRS. Startup scenarios are particularly important as it requires melting of the liquid metal and transiting the HP from sonic limit conditions to a completely operational state.

The B<sub>4</sub>C segments (5 mm thick 120° sectors) in the control drums placed in the radial BeO reflector face the reactor core during launch and startup period, and face 180° away from the reactor core at the end of life. At the beginning of life, the reactor core has an excess reactivity of \$2.12, the 12 BeO/B<sub>4</sub>C control drums in the radial BeO reflector have a total reactivity worth of \$11.64, which is sufficient to operate the reactor through its lifetime with excellent redundancy. This startup scenario was based on a very slow startup that was used for TOPZA-II, due to lack of design data.

## 5.1 REACTOR STARTUP PROCEDURE

The reactivity insertion rate of control drums is of crucial importance to the startup procedure, since it determines the quality of the system startup. In the startup program, reactivity insertion speed is a key parameter and it must be controlled strictly to ensure the reactor period is large than 30 s (Figure 6). When the drums rotate outward at a large speed, the reactor thermal power rises rapidly, reactor period becomes less than 30s. Then the fuel and HP temperature will also exceed the nominal operating temperature. When the drums rotate outward at a slow speed that the reactor would spend a long time to start up and the HP would fail to start up from the frozen state (the HP evaporation rate must be greater than the solidification rate). Perfect startup process is that the reactor thermal power and insertion reactivity would increase gradually in the whole transient, and all parameters do not exceed their corresponding limit.

The simulated startup procedure (Figure 7) to reach nominal operating conditions and supply electric power to the load is ~8450s long. The sequential actions during the startup procedure are:

- 1 Initial state: The temperature of space sink is assumed to be 250K, and the surface emissivity of the radiator is 0.9. The initial temperature of the HP cooled space reactor system is 250K, which is below the melting temperature of sodium (371K). At the beginning of life, the reactor core has an total reactivity of- \$9.52.
- 2 Reactor starts from subcritical to criticality: This phase ends when the total reactivity equals \$0.0. At such time, the reactor power is ~0Wth. The working fluid in HP and AMTEC is still at frozen state.
- 3 Na-HP reaches steady-state : Na-HP starts operation and eventually reaches steady-state. The working fluid in K-HP and AMTEC begin to melt.
- 4 AMTEC and K-HP reach steady-state: AMTEC starts to generate current. AMTEC and K-HP eventually reach steady-state.
- 5 The power of HPS increases and finally reaches to full-power operation.

The next section presents and discusses the calculated transient variation of various operation parameters of the HPS during the startup procedure.

## 5.2 CHANGES IN OPERATION PARAMETERS DURING SYSTEM STARTUP

At the beginning of the startup procedure,  $\sim 0.01W_{th}$  is produced in the reactor core by the radioactive decay of the fuel (Figure 8), while the entire power system is at a uniform temperature of 250K (Figure 9). The reference temperature for the reactivity feedback in the reactor core is taken as 300 K. The BeO/B<sub>4</sub>C drums in the radial reflector rotate outward at a constant angular speed 0.9°/s (Figure 7 point 1~point 2). This phase ends when the total reactivity insertion equals \$0.0 (Figure 7 point 2). The working medium in Na-and K-HP is at frozen state. Although AMTEC is connected during the system startup, but none electric current is generated. Except the reactivity, parameters of HPS have no obvious change. After about 120s from the initiation of the startup procedure, the reactor enters into the second startup phase when the Na-HP begins to melting.

After reactor reaches criticality, the drums rotate outward at an angular speed of 0.003°/s. For the fuel pin temperature changes a little, the temperature reactivity feedback is small that makes the total reactive increase and reaches peak value (point 3 in Figure 7), also reactor thermal power reaches  $\sim 180$  kW<sub>th</sub> (point 1 in Figure 10). When the temperature of the HP exiting the reactor core increases to  $\sim 700$ K (point 1 in Figure 10), the reactor thermal power decreases rapidly. The increasing total reactivity makes reactor thermal power increase, also the heat transfer from fuel pins to HP evaporator. At such time, the Na-HP is at free molecular flow phase, and Na-HP cannot transfer the heat to the condenser. The heat is used only to soar the temperature of Na-HP evaporator and fuel pins. Although Na-HP evaporator temperature increases rapidly, while the Na-HP condenser temperature is kept as 250K which is the initial temperature.

The detailed description of Na-HP startup procedure is described as follows. The freezing temperature for K, typically used in the radiator HPs, and Na, typically used in the reactor HPs is 336K and 371K, respectively. When the average temperature of Na-HP evaporator wall is between 250K and 371K, heat conduction though the wall will melt the working fluid in the evaporator. The vapor pressure is so low that the vapor flow is in a rarefied or free molecular condition. Also working fluid in the wick is still in the solid state in the adiabatic condenser sections of the HP. As the heating continues, the average temperature of Na-HP evaporator wall rises to 708K (The turning point from free molecular period to intermediate period). We can observe that the HP wall temperature rises to 700K and remains almost constant as the sleep temperature front moves along the length of the HP (Figure 10 point 1~point 2). After the uniform hot zone reaches to the condenser end of the HP, the temperature increases to its steady-state value (Figure 10).

When the HP melting front arrives in the condenser side, the Na-HP begins to transfer heat to contacted AMTEC device. Huge temperature ( $\sim 700$ K and 250K) difference makes AMTEC evaporator side temperature rise rapidly (Figure 12 point 1~point 2). The AMTEC condenser side is at freezing state, so there is no working fluid cycling in the liquid-return porous artery and AMTECs cannot generate electric current. There is only radiation heat transfer between the AMTEC evaporator and condenser (Figure 7 point 1~point 3), which results in large temperature difference between evaporator and condenser. The heat conduction between the AMTEC condenser and radiator evaporator make the radiator evaporator temperature increase.

The outward rotation of the control drums during the third phase (0.001°/s) is slower than that during the second phase (Figure 7 point 3~point 4). This phase ends at 8450s, or 6850s after the second startup phase, when the total external reactivity insertion reaches \$0.7748 (Figure 7).

When the high and low pressure cavity of AMTEC produces enough pressure difference, the BASE begins to generate electric current. The additional affiliated heating loss has risen sharply, a large amount of heat transfer into the low pressure cavity and meanwhile AMTEC cold side temperature increases rapidly (Figure 12 point 3~point 5). With AMTEC started (4000s), AMTEC hot and cold side temperature increases rapidly (Figure 12 point 4~point 6), also the Na-HP and the fuel temperature. Soon the second reactor thermal power peak appears (Figure 8). At the end of the third phase of the startup procedure ( $\sim$

8000s), the reactor thermal power reaches ~420KW (point 3 in Figure 8).

Around 9000s after the reactor startup, AMTECs start generating current (Figure 11), and HPs work in the steady-state (Figure 10). The total reactivity is nearly zero, as the external and feedback reactivity is equal in magnitude and opposite in sign (point 4 in Figure 7). The redundant reactor thermal power is released to the environment by the radiator.

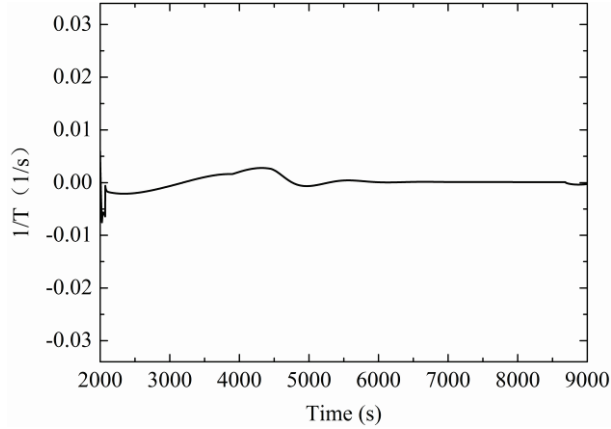


Figure 6 The reactor period (T)

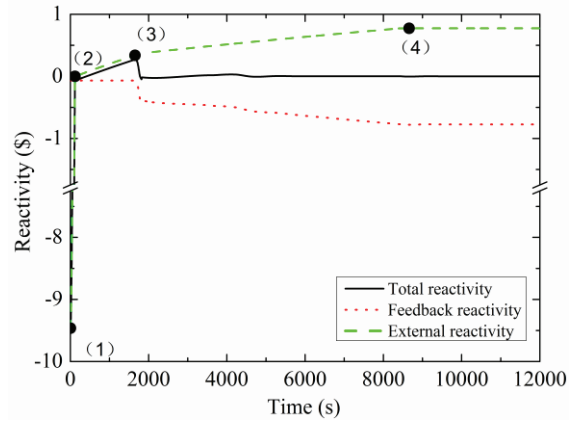


Figure 7 Reactivity variation during startup

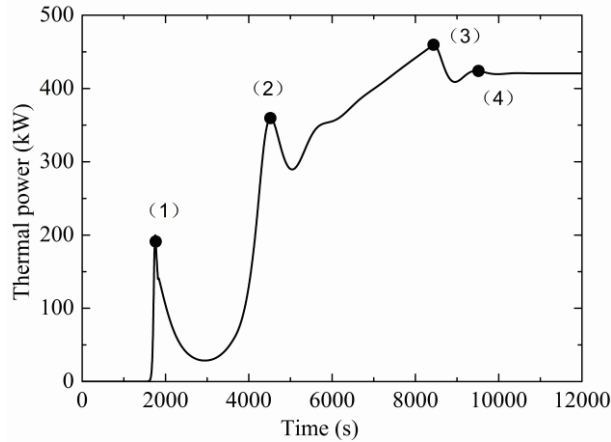


Figure 8 Calculated thermal power temporal profile during startup

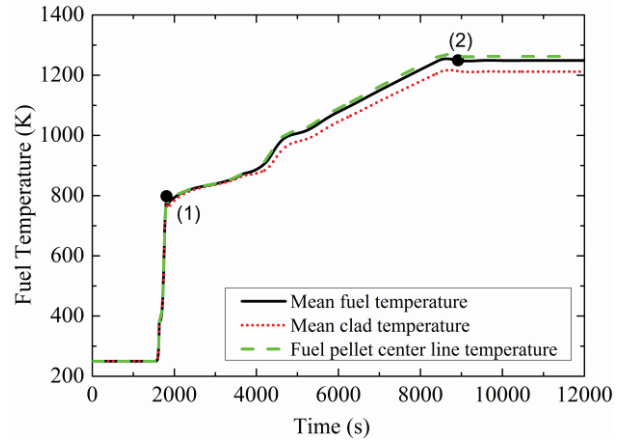


Figure 9 Calculated fuel temperature temporal profile during startup

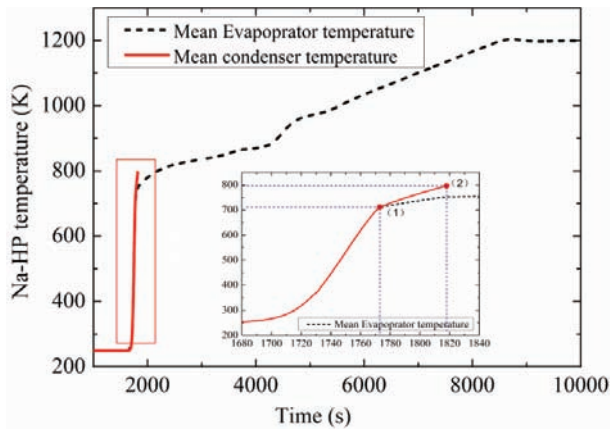


Figure 10 Calculated Na-HP temperature temporal profile during startup

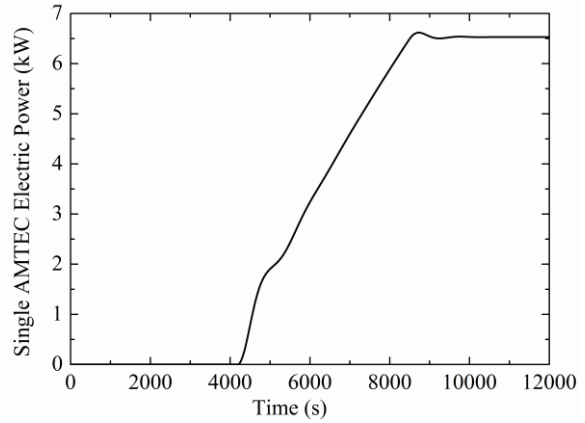


Figure 11 Calculated AMTEC electric power temporal profile during startup

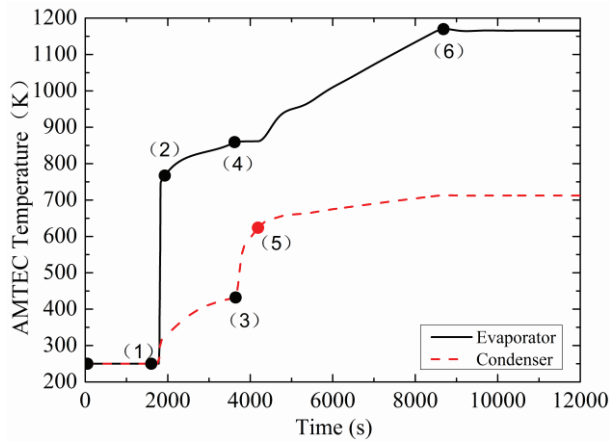


Figure 12 Calculated AMTEC temperature temporal profile during startup

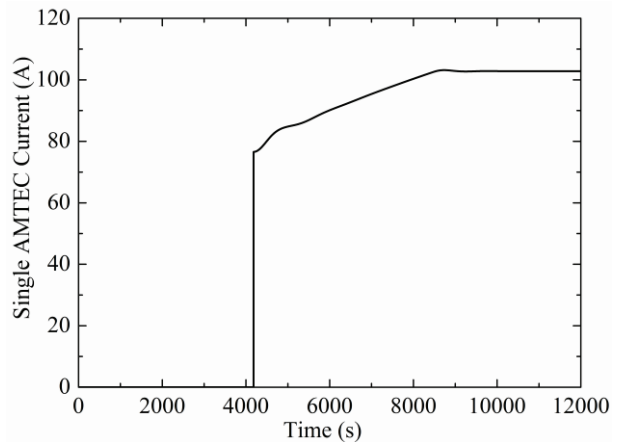


Figure 13 Calculated AMTEC electric current temporal profile during startup

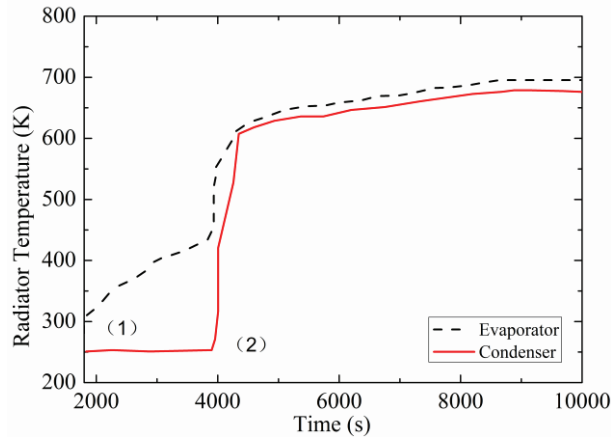


Figure 14 Calculated radiator temperature temporal profile during startup

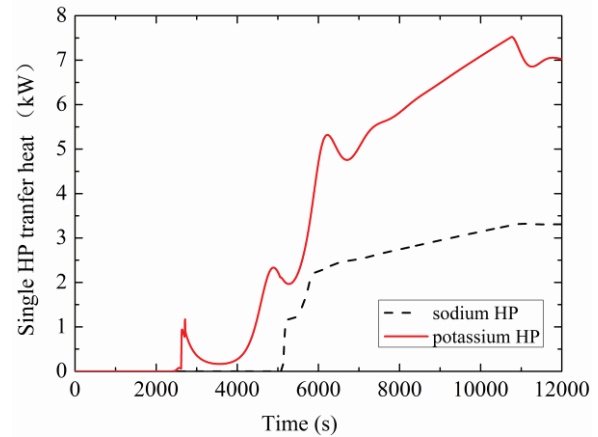


Figure 15 Calculated single HP transfer heat temporal profile during startup

## 6 CONCLUSION

This paper introduces a system code (TAPIRS) capable of modeling the HPS. This system code is capable of modeling coupled the reactor kinetics phenomena, heat transfer dynamics within the fuel pins, the transient behavior of HP (including the melting of the working fluid), the generation of voltage and current in the AMTEC, the radiator. The reactor starts up from subcritical state to full power state which show that the reactor can start by the nuclear heat.

## 7 REFERENCES

1. El-Genk, M.S., *Space Nuclear Reactor Power System Concepts with Static and Dynamic Energy Conversion*. Energy Conversion and Management, 2008. **49**(3): p. 402-411.
2. El-Genk, M.S. and J.-M. Tournier, "SAIRS"-Scalable Amtec Integrated Reactor space power System. Progress in nuclear energy (New series), 2004. **45**(1): p. 25 - 69.
3. Poston, D.I., R.J. Kapernick, and R.M. Guffee. *Design and Analysis of the SAFE-400 Space Fission Reactor*. in *AIP Conference Proceedings*. 2002.
4. Tournier, J.-M. and M.S. El-Genk. *Reactor Lithium Heat Pipes for HP-STMCs Space Reactor Power System*. in *AIP conference proceedings*. 2004.
5. Wu, S.-Y., L. Xiao, and Y.-D. Cao, A Review on Advances in Alkali Metal Thermal to Electric Converters (AMTECs). International Journal of Energy Research, 2009. **33**(10): p. 868-892.
6. El-Genk, M.S., *DynMo-TE: Dynamic Simulation Model of Space Reactor Power System with Thermoelectric Converters*. Nuclear engineering and design, 2006. **236**(23): p. 2501-2529.
7. King, J.C. and M.S. El-Genk, *Thermal-Hydraulic and Neutronic Analyses of the Submersion-Subcritical, Safe Space (S4) Reactor*. Nuclear Engineering and Design, 2009. **239**(12): p. 2809-2819.
8. Wright, S.A. and M. Houts. *Coupled Reactor Kinetics and Heat Transfer Model for Heat Pipe Cooled Reactors*. in *AIP Conference Proceedings*. 2000.
9. Ran, X., et al., *Safety Characteristic Analysis of Advanced Space Fast Reactor (In Chinese)*. Atomic Energy Science and Technology, 2006. **4**(6).
10. Waltar, A.E. and A.B. Reynolds, *Fast Breeder Reactors*. 1981, New York: Pergamon Press. xxvi, 853 p.
11. Yuan, H. and D. Hu, *High-Order End Floating Method-for Solving Point Reactor Neutron Kinetics Equations (In Chinese)*. Nuclear Power Engineering, 1993. **14**(2): p. 122-128.

12. Wulff, W. *Lumped-Parameter Models for Transient Conduction in Nuclear Reactor Components*. in *U.S. Nuclear Regulatory Commission*. 1980. Brookhaven National Lab., Upton, NY (USA).
13. Cao, Y. and A. Faghri, *A Numerical Analysis of High-Temperature Heat Pipe Startup from the Frozen State*. *Journal of heat transfer*, 1993. **115**(1): p. 247-254.
14. Ochterbeck, J., *Modeling of Room-Temperature Heat Pipe Startup from the Frozen State*. *Journal of thermophysics and heat transfer*, 1997. **11**(2): p. 165-172.
15. Zuo, Z. and A. Faghri, *A Network Thermodynamic Analysis of the Heat Pipe*. *International Journal of Heat and Mass Transfer*, 1998. **41**(11): p. 1473-1484.
16. Bushman, A., et al., *The Martian Surface Reactor: An advanced nuclear power station for manned extraterrestrial exploration*, 2004, MIT-NSATR-003, Cambridge.
17. Tournier, J.-M. *An Analytical Model for Liquid-Anode and Vapor-Anode AMTEC Converters*. in *Space technology and applications international forum (STAIF-97)*. 1997. AIP Publishing.
18. Staub, D., *SNAP 10A Summary Report*. *Atomics International Report NAA-SR-12073*, March, 1967. **25**.
19. Makarov, A.N., et al. *The Operating Regimes and Basic Control Principles of SNPS "TOPAZ"*. in *Proceedings of the eighth symposium on space nuclear power systems*. 2008. AIP Publishing.
20. Yuan Yuan, S.J., *Transient Analysis of Heat Pipe Cooled Space REactor Power System*, X.J. University, Editor 2014.